Analytical Transient Two-Phase Model For Dry-Superheated Debris Bed Under Top Flooding Conditions

Alejandro Villarreal Larrauri, Renaud Meignen, Michel Gradeck, Nicolas Rimbert

ANALYTICAL TRANSIENT TWO-PHASE MODEL FOR DRY-SUPERHEATED DEBRIS BED UNDER TOP FLOODING CONDITIONS

Alejandro Villarreal Larrauri, Renaud Meignen
Institut de Radioprotection et de Sûreté Nucléaire (IRSN)
13115, St. Paul lès Durance, France
alejandro.villarreallarrauri@irsn.fr; renaud.meignen@irsn.fr

Michel Gradeck, Nicolas Rimbert
Laboratoire d'Énergétique et de Mécanique Théorique et Appliquée (LEMTA)
Université de Lorraine, CNRS
2 Avenue de la Forêt de Haye, BP160, 54504 Vandoeuvre les Nancy
michel.gradeck@univ-lorraine.fr; nicolas.rimbert@univ-lorraine.fr

ABSTRACT

In a severe accident, during a Molten Corium-Concrete Interaction under water (MCCI) corium may be found in two expected configurations: a layer of millimetric particles with an intrinsic morphology (debris bed) or a compact fractured crust of solidified corium. This paper presents the work done to assess cooling capabilities of corium in the aforementioned configurations. The work is carried out using a CFD code (MC3D) and by developing an analytical model. Experimental studies suggest that the debris bed quenching is a two-stage process where, at first, the water penetrates the bed through preferential channels (water fingering), leaving temporarily some parts of the bed dry and unquenched. However, the precise characterization of water fingering is not clear. The CFD calculations expressly indicate that the water penetrates the porous media through the fingers as a local 2-phase flow with relatively high void saturation. The analytical model provides explanations for this flow configuration, given the debris bed characteristics (size and distributions of the particles composing it), indicating that it corresponds to the critical vapor flow conditions beyond which 2-phase flow is impossible. Special focus is given to the particular configuration of a compact fractured crust of a re-solidified corium pool. Given the fracture characteristics, the analytical model compares well with the results of the dedicated SSWICS tests.

KEYWORDS
Severe accidents, Top flooding, Debris bed cooling, Porous media

1. INTRODUCTION

In case of severe accident with partial or extensive reactor core meltdown, the superheated magma made of molten steel and fuel (corium) may threaten the integrity of both the reactor vessel (in-vessel) and the reactor containment building (ex-vessel), if long-term coolability is not assured. Depending on the scenario, corium may be found in two expected configurations: a layer of millimetric particles with an intrinsic morphology (debris bed) or a compact fractured crust. For both configurations, the layer is expected to be initially at an elevated temperature (>1600 K), and to contain radioactive material that would generate heat as their fission products decay. To mitigate the consequences of the accidental progression, water is injected to stabilize the material. If the heat generated in these structures is higher than a certain limit, it may induce re-melting and hinder/delay the stabilization of the accidental progression by the safety water injection mechanism. In the context of severe accidents, for both configurations, some experimental studies have been made to investigate their cooling capabilities. Firstly, for debris bed, two kinds of experimental studies have been carried out: dry-out and re-flooding experiments. Dry-out experiments are quite abundant and

have explored a variety of different parameters such as particle size, pressure, materials, size of debris bed, and shape of debris bed, amongst others. On the contrary, re-flooding experiments for initially hot and dry debris bed in top flooding configuration, as expected in accidental scenario, have been seldom performed (principally by Ginsberg et al. [1] and Cho et al. [2]), and the phenomenology not thoroughly studied. For fractured crusts, even fewer dedicated experiments have been made. The Small Scale Water Ingression and Crust Strength (SSWICS) tests [3] were designed specifically with the objective to study the Water-Ingression (W-I) phenomena, i.e. the percolation of water through cracks in the fractured crust.

Analogous studies in other fields, such as, petroleum engineering, hydrogeology, geophysics, amongst others, have investigated comparable phenomena like gravitational water fingering in porous media without heating. However, the understanding of such process "is deficient in determining the field conditions where gravity fingering can be expected and the behavior of the field-scale fingering process when it occurs"[4]. Nonetheless, analytical and experimental evidence of the 2D two-phase water penetration from these studies can be useful in drawing parallels to the configurations expected in the context of corium cooling.

Classical models used for evaluating the W-I phenomena through fractured crust include Jones model [5]:

$$\phi_{Jones} = \mathrm{K}\frac{\mathrm{h_{lv}}(\rho_l-\rho_v)\mathrm{g}}{2\left(\frac{\mu_v}{\rho_v}\right)} \quad \textbf{(1)}$$

where, $\Phi\left[\frac{\mathrm{W}}{\mathrm{m^2}}\right]$ is the heat flux extracted at the surface, K [$\mathrm{m^2}$] is the absolute permeability, ρ_i $\left[\frac{\mathrm{kg}}{\mathrm{m^3}}\right]$ is the density of phase "i"(l: liquid; v: vapor), μ_i $\left[\frac{\mathrm{kg}}{\mathrm{m\cdot s}}\right]$ is the kinematic viscosity of phase "i", $\mathrm{g}\left[\frac{\mathrm{m}}{s^2}\right]$ the gravitational acceleration, and $\mathrm{h_{lv}}\left[\frac{\mathrm{J}}{\mathrm{kg}}\right]$ the latent heat of vaporization.

Another model to evaluate the heat extracted during the W-I phenomena is Lister-Epstein model [6]:

$$\phi_{LE} = \left[\frac{\mathrm{h_{lv}}(\rho_l-\rho_v)\mathrm{g}}{12\sqrt{2}\left(\frac{\mu_v}{\rho_v}\right)}\right]^{\frac{5}{13}} [\beta_{cr}(\mathrm{T_{cr}}-\mathrm{T_{sat}})]^{\frac{15}{13}} \left[\frac{32\alpha_{cr}{}^2\mathrm{NL}\rho_{cr}{}^2\left[h_{f,cr}+c_{\mathrm{p,cr}}(T_{cr,sol}-T_{sat})\right]^2}{T_{cr,sol}-T_{cr}+\frac{h_{f,cr}}{\mathrm{c_{p,cr}}}}\right]^{\frac{4}{13}} \quad \textbf{(2)}$$

where, ρ_{cr} $\left[\frac{\mathrm{kg}}{\mathrm{m^3}}\right]$ is the density of the crust material, $\mathrm{h_{cf,cr}}\left[\frac{\mathrm{J}}{\mathrm{kg}}\right]$the latent heat of fusion of the crust, $\mathrm{c_{p,cr}}$ $\left[\frac{\mathrm{J}}{\mathrm{kgK}}\right]$ the heat capacity of the crust, α_{cr} $\left[\frac{\mathrm{m^2}}{\mathrm{s}}\right]$ the thermal diffusivity of the crust, β_{cr} $\left[\frac{1}{\mathrm{K}}\right]$ the coefficient of linear expansion of the crust, $\mathrm{T_i}$ [K] temperature of "i" (cr: crust; cr,sol: solidification of the material that constitutes the fractured crust), L[-] Lister parameter, and N [$\mathrm{K\ m^{1/2}}$] a numerical constant of the model. Lister-Epstein model is based on a theory of crack propagation in rocks, which estimates a permeability K from a series of physical properties of the material constituting the crust, and the fluids involved in the cooling. Lister-Epstein model also uses a hydrodynamic term based on Jones that may not account properly the effects for pressure.

This paper is divided into several sections that focus on different aspects of the phenomenology in question. Firstly, the next section presents the results of the evaluation of re-flooding of a hot-dry debris bed performed with the use of a 3D thermal-hydraulic multiphase flow CFD code, called MC3D that highlights the occurrence of a 2D two-phase water penetration. The analysis of the phenomenology based on, initially, an analytical steady debris bed model that gives insight into the conditions that govern the flow in such

configuration is presented in section 3. Following, the extension of the steady-state model towards a 1D model and the comparison with both simulations and the Ginsberg experimental data is introduced in section 4. Lastly, the application of such model in the case of a fractured porous media and its comparison with the experimental data, in the context of the W-I phenomena are given in section 4.3.

2. EVALUATION OF FLOODING WITH MC3D

The capabilities of MC3D regarding the modeling of debris bed coolability were investigated in [7] and [8], and deemed adapted to the applications such as the one of the present study. The question of top re-flooding was partially discussed in [7] and will therefore be examined more precisely here. The MC3D code [9] is devoted to multiphase thermal-hydraulic flow studies and evaluations in the field of nuclear safety. Its major use currently concerns the evaluation of (molten) Fuel Coolant Interaction (FCI) in power and experimental reactors. Two models describing the premixing (PREMIX) and the explosion (EXPLO) stages were developed. Various options for evaluating frictions in a debris bed are available in the PREMIX model, which is thus used here. The MC3D code is based on an Eulerian two phase approach with each component/mixture described by conservation equations (mass, momentum and energy.) These balance equations are solved with a semi-implicit method. A staggered grid is used (Cartesian or cylindrical) where velocities are expressed at the faces and other variables at the center of meshes. The set of available frictional laws, in MC3D, is relatively large and accounts for the interfacial frictions which become important for large particles. Nevertheless, the capillary effects have not yet been incorporated, due to the fact that the current applications of the code do not require it. The impact of capillarity will be discussed in section 3.3.

In this study, the major interest of using MC3D is for the situation of re-flooding of a dry debris bed. Due to the limited number of available data, and lack of understanding, re-flooding of debris bed is a particular challenge. Ginsberg et al. [1] provided a detailed study with re-flooding experiments using debris bed of round spheres of diameters ranging from 0.89 to 12 mm. He could observe that the flooding occurred in two stages. In a first step, the liquid enters the bed by vertical channels therefore leaving zones of dry particles. For given conditions, the velocity of downward cooling front is constant even if it is a function of the particle diameter and the initial bed temperature. When the front reaches the bottom of the bed, the water fills the bottom of the test section and uniformly fills the debris bed upwards. The upward front is fed by the water flowing down through the zones already "cold" and cools the remaining dry pockets. The velocity of this upward front is also constant. It is important to note that the rate of steam production remains approximately constant during the whole process (downward and upward flow steps). The apparent propagation of the downward front as fingers may be a similar process to the one regularly observed in the downward penetration of water in porous medium, referred to as Saffman-Taylor instabilities [10]. However, in the context of re-flooding of a hot debris bed, the Saffman-Taylor model does not apply.

An illustration of a typical calculation of a Ginsberg experiment is given in Figure 1. It is noticeable that the downward flow proceeds mainly as fingers, thus following, at least qualitatively, the configuration depicted by Ginsberg et al. As expected, the bed is cooled only in the re-flooded regions. An important outcome of these calculations is that, in contrast with the hypotheses pictured by Ginsberg et al. [1], the flooded regions are not saturated in water, but diphasic, with a rather low liquid saturation, about 25 %.
What is also clear is the impact of the meshing since the fingers seem to follow columns of cells. Although the mesh sensitivity is found acceptable for preliminary studies, it is obvious that physical process of cooling needs to be further investigated in order to improve the capabilities of the model. A first issue is to understand what drives the flow saturation in the flooded fingers. The analytical work summarized in the following sections allows a first explanation, and thus may justify the behavior of the code. The second issue is to characterize the instability of the flow and the geometric characteristics of the fingers (e.g. wave length). This is out of the scope of the present paper. The results of MC3D simulations and indications of their validity will be discussed in section 4.

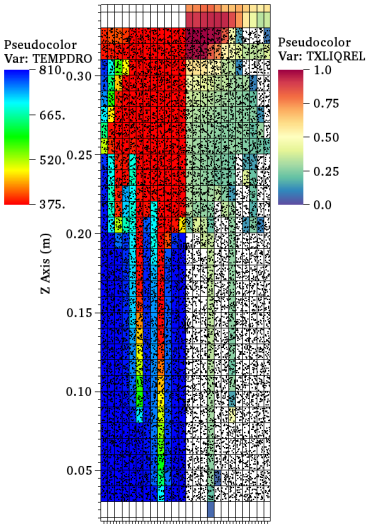

Figure 1. MC3D simulation of an experimental case from Ginsberg et al. [1] (T_0 = 810 K, d_p=3,2 mm). Debris bed: black dots. Right : liquid saturation. Left : temperature map of the steel spheres.

3. CRITICAL HEAT FLUX IN FLOODED DEBRIS BEDS

3.1. Introduction

For 1D two-phase flow in steady conditions, the pressure loss for phase "i" in a porous medium is generally approximated by:

$$-\frac{\partial P_i}{\partial z}=\rho_i g+\frac{\mu_i}{K K_{r,i}} j_i+\frac{\rho_i}{\eta \eta_{r,i}}|j_i| j_i+\begin{cases}\frac{F_{lv}}{\alpha}, & i=v\\ \frac{F_{lv}}{1-\alpha}, & i=l\end{cases}+\frac{\partial P_c}{\partial z} \qquad (3)$$

where $j_i\left[\frac{m}{s}\right]$ is the superficial velocity of phase "i", η [m] is the absolute passability [11], $K_{r,i}$ [-] and $\eta_{r,i}$ [-] the relative permeabilities and passabilities for 2-phase flow conditions, $\frac{\partial P_c}{\partial Z}\left[\frac{kg}{m^2 \cdot s^2}\right]$ is the pressure drop due to capillary effects, and $F_{lv}\left[\frac{kg}{m^2 \cdot s^2}\right]$ the interfacial friction factor.

As proposed by Ergun [12], the porous media parameters K and η in a bed of solid round particles, can be evaluated with:

$$K=\frac{\varepsilon^3 d_p{}^2}{150(1-\varepsilon)^2}, \qquad \eta=\frac{\varepsilon^3 d_p}{1.75(1-\varepsilon)}=\frac{\sqrt{150}\cdot\varepsilon^{3/2}}{1.75}\sqrt{K} \qquad (4)$$

where d_p [m] is the Sauter mean diameter of the debris bed constituents (spheres) [11], and ε [-], is the porosity. For non spherical particles, an additional parameter may be necessary to calculate the

representative diameter. However, in the present work, the porous media (debris, or crust), will be characterized by their permeability and passability.

The two-phase liquid/gas interfacial frictions become important only at large permeabilities, mostly beyond the scope of the present work, and will be therefore neglected. Although several relations are available to calculate the relative permeability and passability, most of them take the following form given in **Table I** :

Table I. Relative Permeabilities and Passabilities and coefficients

Phase	$K_{r,i}$	$\eta_{r,i}$
Liquid	$(1-\alpha)^n$	$(1-\alpha)^m$
Vapor	$(\alpha)^n$	$(\alpha)^m$

Author	n	m
Lipinski 1982 [13]	3	3
Reed [14]	3	5
Hu&Theofanous [15]	3	6

For fractured porous media, many other formulas have been developed to calculate the relative permeability of both phases; some of them are presented and discussed in section 4.3.

The capillary effects become important at very small permeabilities (K<1E-9 m^2), i.e. likely in fractured crust. For simplicity, at first, in order to establish a method they are not taken into account .They will be the subject of a specific discussion in section 3.4.

3.2. Laminar Regime

First, only laminar effects are considered. At each height Z, and neglecting the gravitational effects in the gas, the pressure gradient is assumed common to all phases, and is expressed as follows:

$$-\frac{\delta P_i}{\delta z}=\frac{\mu_v}{KK_{r,v}}j_v=\frac{\mu_l}{KK_{r,l}}j_l+\rho_l g \qquad \textbf{(5)}$$

In steady state condition, there is no mass accumulation and thus the upward vapor flux is equal to the downward liquid flux, and is formulated as:

$$\rho_v j_v=-\rho_l j_l \qquad \textbf{(6)}$$

Substituting eq.(6) into eq.(5) (i.e. balancing mass fluxes, viscous shear and gravity) yields the following relationship :

$$j_v=\frac{\frac{\rho_l}{\rho_v}Kg}{\left(\frac{\mu_v}{\rho_v K_{r,v}}+\frac{\mu_l}{\rho_l K_{r,l}}\right)} \qquad \textbf{(7)}$$

Using the formulations of the relative permeabilities, the gas flux can be linked to local void saturation. The result is shown in Figure 2 at different pressures for a representative debris bed with d_p=1mm and ε=0.4, evaluating the properties at saturation temperature. As can be seen, for any given j_v, there are two possible values for α, i.e. two physical configurations, and a maximum, located at void saturation between

0.5 and 0.75. The maximum represents then a critical flux beyond which 2-phase flow is unstable (and, likely, not possible).

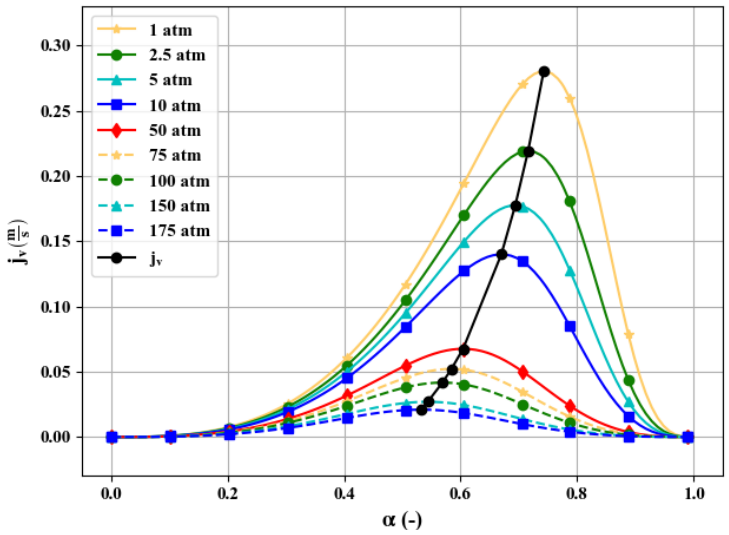

Figure 2. Laminar j_v as a function of the vapor saturation for different pressures, K~1.20E-10 m^2

This critical point can be obtained analytically, resulting in

$$\alpha_{l,crit}=\left[1+\left(\frac{\mu_l}{\mu_v}\frac{\rho_v}{\rho_l}\right)^{\frac{1}{n+1}}\right]^{-1} \approx 0.743 \text{ (@ 1 atm and n=3)} \tag{8}$$

$$j_{v,lcrit}=\frac{\frac{\rho_l}{\rho_v}Kg}{\frac{\mu_v}{\rho_v\left[1+\left(\frac{\mu_l}{\mu_v}\frac{\rho_v}{\rho_l}\right)^{\frac{1}{n+1}}\right]^{-n}}+\frac{\mu_l}{\rho_l\left[\frac{\left(\frac{\mu_l}{\mu_v}\frac{\rho_v}{\rho_l}\right)^{\frac{1}{n+1}}}{1+\left(\frac{\mu_l}{\mu_v}\frac{\rho_v}{\rho_l}\right)^{\frac{1}{n+1}}}\right]^{-n}}} \tag{9}$$

Now, a critical heat flux can be determined. In the heated debris bed, at each elevation Z, the vapor flux comes from the vaporization of the water below Z due to volumetric power. In the case of saturated water, as expected, this vaporization exactly balances the input energy below Z:

$$\rho_v j_v(z)=\frac{1}{h_{lv}}\int_0^Z P_v dz=\frac{P_v Z}{h_{lv}}\equiv\frac{\phi}{h_{lv}}$$

$$\phi=\rho_v j_v h_{lv} \tag{10}$$

Incorporating eq. (7) in eq.(10) yields a relationship between the input power and the local vapor saturation in the terms of relative permeabilities, which in the laminar case can be expressed as:

$$\phi_l = \frac{\rho_l g K h_{lv}}{\left(\frac{\mu_v}{\rho_v K_{r,v}} + \frac{\mu_l}{\rho_l K_{r,l}}\right)} = \frac{\rho_l g K h_{lv}}{\left(\frac{\mu_v}{\rho_v \alpha^n} + \frac{\mu_l}{\rho_l (1-\alpha)^n}\right)} \quad \textbf{(11)}$$

The critical flux is obtained by evaluating eq.(11) at $j_{v,l}$, hence at $\alpha = \alpha_{l,crit}$, which would result in:

$$\phi_{l,crit} = \frac{\rho_l g K h_{lv}}{\frac{\mu_v}{\rho_v}\left[1+\left(\frac{\mu_l}{\mu_v}\frac{\rho_v}{\rho_l}\right)^{\frac{1}{n+1}}\right]^n + \frac{\mu_l}{\rho_l}\left[\frac{1+\left(\frac{\mu_l}{\mu_v}\frac{\rho_v}{\rho_l}\right)^{\frac{1}{n+1}}}{\left(\frac{\mu_l}{\mu_v}\frac{\rho_v}{\rho_l}\right)^{\frac{1}{n+1}}}\right]^n} \quad \textbf{(12)}$$

Comparing eq.(11) with Jones model eq.(1), the difference comes from the denominator. It provides a correction regarding the impact of the pressure by including the viscous terms for the liquid phase, which is not the case for Jones model. It is noticed that the maximum (critical) heat flux does not occur at void saturation tending to 1, but quite far below. This is due to the fact that the superficial velocity is maximal when the sum of the liquid and vapor viscous contributions are minimal. It may also be noticed that, below critical conditions, two 2-phase flow configurations are possible. This may induce some instability of the flow.

3.3. Inertial Regime

One can follow the same procedure for inertial flow conditions, with the momentum balance being:

$$\frac{\rho_v}{\eta\eta_{r,v}}|j_v|j_v = \frac{\rho_l}{\eta\eta_{r,l}}|j_l|j_l + \rho_l g \quad \textbf{(13)}$$

which leads to the critical conditions $\alpha_{i,crit}$ and $\phi_{i,crit}$:

$$\alpha_{i,crit} = \left[1+\left(\frac{\rho_v}{\rho_l}\right)^{\frac{1}{m+1}}\right]^{-1} \quad \textbf{(14)}$$

It is noticed that, in the case of debris beds, the passability is a function of ε and K (eq.(4)) and so the critical flux can be expressed in term of K:

$$\phi_{i,crit} = \sqrt{\frac{\rho_v \rho_l \frac{\sqrt{150}}{1.75}\varepsilon^{\frac{3}{2}}\sqrt{K} g h_{lv}^{\,2}}{\left[1+\left(\frac{\rho_v}{\rho_l}\right)^{\frac{1}{m+1}}\right]^{m+1}}} \quad \textbf{(15)}$$

It is possible to build an analytical solution to the full problem, but a sufficient approximation is obtained by merging $\phi_{l,crit}$ and $\phi_{i,crit}$ as follows:

$$\phi_{crit}=\min\left(\phi_{l,crit},\phi_{i,\,crit}\right) \tag{16}$$

3.4. Capillary Effects

Capillary effects, which arise from the pressure difference across the curved interface between two immiscible fluids, may condition, or modify the way the phases flow in the porous media. Dullien et al. [16] presented, amongst others, some experimental measurements highlighting the existence of a hysteresis between cases for water imbibition ("the displacement of the non-wetting phase by the wetting phase"[17]) and drainage (non-wetting phase replacing the wetting phase). To account for the complex effects of capillarity in porous media several approximate solutions have been proposed. To evaluate the capillary pressure, a rather common correlation was formulated by Leverett [18] dependent on the porous media characteristics and an effective saturation function, presented here as:

$$P_C=P_G-P_L=\sigma_{LG}\cos(\theta)\sqrt{\frac{\varepsilon}{K}}J(S^*) \tag{17}$$

with $\sigma_{LG}\left[\frac{N}{m}\right]$ being the liquid-vapor surface tension (calculated at T_{sat}), and θ [°] the wetting angle (here taken as 0 to maximize the function). $J(S^*)$ [-] is a non-dimensional expression called the Leverett J-function dependent of S^* [-] the effective liquid saturation, both of which may be evaluated using the equations given in **Table II** where S_{ir} and S_{irg} are the irreducible liquid and gas saturation (here both taken as 0.05).

Table II. Common expressions for Leverett J function and Effective saturation

Correlation	Expression
Effective saturation[18]	$S^*=\frac{(1-\alpha)-S_{ir}}{1-S_{irg}-S_{ir}}$
J(S*) – Udell [19]	$1.417\left(1-S^*\right)-2.12\left(1-S^*\right)^2+1.263\left(1-S^*\right)^3$
J(S*) – van Genuchten [20]	$\frac{1}{5}\left(S^{*-\frac{1}{5}}-1\right)^{\frac{1}{0.8}}$
J(S*) – Turland & Moore	$1.5-9.2S^*+\frac{88}{3}S^{*2}-\frac{880}{27}S^{*3},\ 0\le S^*<0.3$ $0.62-0.4S^*,\ 0.3\le S^*<0.8$ $14.7-53.2S^*+66S^{*2}-\frac{55}{2}S^{*3},\ 0.8\le S^*\le 1.0$

Reformulating previous expressions to include the capillary effects can be done by adding eq.(17) into the momentum balance equations (eq.(3)) and linearizing the term $\frac{\delta P_c}{\delta z}$ over the entire length of the debris bed Z [m] by $\frac{\delta J(S^*)}{\delta z}=\frac{\Delta J(S^*)}{Z}$ for simplicity. This leads to a corrective to be multiplied for the previous laminar and inertial critical fluxes such that:

$$\phi_{lcap,crit}=\phi_{l,crit}\left(1+\frac{\sigma_{LG}\cos(\theta)\sqrt{\frac{\varepsilon}{K}}\Delta J(S^*)}{\rho_l g Z}\right) \quad (18)$$

$$\phi_{icap,crit}=\phi_{i,crit}\sqrt{1+\frac{\sigma_{LG}\cos(\theta)\sqrt{\frac{\varepsilon}{K}}\Delta J(S^*)}{\rho_l g Z}} \quad (19)$$

At the bottom, the effective saturation is null, and so the Leverett function. Hence $\Delta J(S^*)$ can be approximates as $J(S^*)$, the latter being evaluated at α. It is noticed that the formulation introduces an additional parameter which is the height Z of the bed (or height of the critical point).

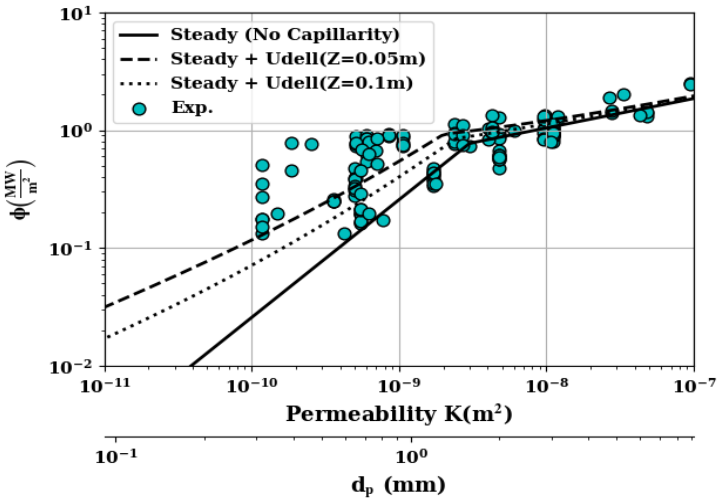

Figure 3. ϕ_{Steady} as a function of permeability compared to the experimental data

Figure 3 plots the derived critical heat flux as a function of permeability (with the approximate corresponding d_p in the secondary x-axis underneath) evaluated at either $\alpha_{i,crit}$ or $\alpha_{i,crit}$ against experimental data. The dots plot a series of different dry-out experiments with similar configuration (cylindrical test section, atmospheric pressure, water injection from the top, initially flooded debris bed, injected water temperature at/close to saturation temperature, steel particles) from Hofmann [21], Miyazaki et al. [22], Barleon et al. [23], Atkhen & Berthoud [24], Squarer et al. [25], amongst other taken from Lipinski [13] (Barleon & Werle, Gabor &Cassulo, Dhir & Catton, Keowin, Gabor et al., Somerton et al., Trenberth & Stevens, Squarer & Peoples, and Sowa). The debris bed heights ranged from 0.02 m to 0.64 m with a mean of 0.15 m. The solid black curve plots eq.(16) without capillary effects, whilst both the dotted and the dashed black lines considers capillary effects using the Udell formulation for two different debris bed heights.

Despite simplifications, formulation seems sufficiently accurate for the inertial regime. In the laminar regime, the situation is much more complex as the proposed formulation seems to give a minimum. The large scatter of experimental result is in general attributed to the fact that, in such conditions, the actual characteristics of the debris bed, notably the permeability, are often uncertain, as they may be modified by

the flow forces themselves [22]. At low values of bed height, this last may drastically modify the initial conditions giving rise to experimental scatter. Nevertheless, the capillary effects are perceptible, although they are still largely within the scatter.
The use of the different correlations presented in **Table II** leads to changes that are moderate and still within the uncertainties. Thus, the Udell formulation, the simplest, will be used henceforth.

4. UNSTEADY 1D PENETRATION MODEL

4.1. Derivation of the Model

Assuming that the flow below the front is steady, that the front has no thickness (sharp front), and that along Z the energy is entirely converted into latent heat of vaporization (total equilibrium of liquid and water vapor), the effective heat flux balance can be expressed as:

$$j_v\rho_v=\frac{1}{h_{lv}}\left[\phi_z+u(1-\varepsilon_0)\rho_d c_{p,d}\Delta T\right] \tag{20}$$

with $\phi_z = P_v Z \ \left[\frac{MW}{m^2}\right]$, $c_{p,d}\ \left[\frac{J}{kgK}\right]$ the heat capacity of the material that constitutes the debris bed , ΔT [K] being the temperature difference between the initial temperature of the debris bed, T_0, and T_{sat}, ε_0 [-] the porosity at the lower boundary, and u $\left[\frac{m}{s}\right]$ the velocity of the cooling front.

It is important to note that if the front progresses, there would be a non-equilibrium in the mass balance since a mass fraction, here called, X_{H20} $[-]$ would be used to fill (partially) the empty pores below the front, hence eq.(6) can be rewritten as:

$$\rho_v j_v+\rho_l\left(j_l+(X_{H_2O})u\varepsilon_0\right)=0 \tag{21}$$

In the laminar regime, solving for the vapor superficial velocity j_v using eq.(21), and eq.(3) (laminar term for the vapor phase, laminar, gravitational and capillary term for the liquid phase) results in:

$$j_v=\frac{\frac{\rho_l}{\rho_v}gK}{\left(\frac{\mu_v}{\rho_v K_v}+\frac{\mu_l}{\rho_l K_{r,l}}\right)}\left(1-\frac{\mu_l}{\rho_l}\frac{\varepsilon_0}{KK_{r,l}}\frac{X_{H_2O}u}{g}+\frac{\sigma_{LG}\cos(\theta)\sqrt{\frac{\varepsilon}{K}}\Delta J(S^*)}{\rho_l gZ}\right) \tag{22}$$

From eq.(20) and eq.(22), u can be expressed as:

$$u_{lam}=\frac{\rho_l gKK_{r,l}h_{lv}\left(1+\frac{\sigma_{LG}\cos(\theta)\sqrt{\frac{\varepsilon}{K}}\Delta J(S^*)}{\rho_l gZ}\right)-\phi_z K_{r,l}\left(\frac{\mu_v}{\rho_v K_v}+\frac{\mu_l}{\rho_l K_{r,l}}\right)}{\mu_l X_{H_2O}\varepsilon h_{lv}+(1-\varepsilon_0)\rho_d Cp_d\Delta TK_{r,l}\left(\frac{\mu_v}{\rho_v K_{r,v}}+\frac{\mu_l}{\rho_l K_{r,l}}\right)} \tag{23}$$

For the inertial regime, as seen previously, the capillary pressure effect can be neglected. Following the same approach as before, the front velocity u is given by the 2 equations below (that can be solved numerically without major difficulties):

$$j_v = \frac{1}{\rho_v \eta_l} \frac{(1-\alpha)\varepsilon_0 u}{\left(\frac{1}{\rho_v \eta_v} + \frac{1}{\rho_l \eta_l}\right)} \left(1 \pm \left[1 - \rho_v \eta_l \left(\frac{1}{\rho_v \eta_v} + \frac{1}{\rho_l \eta_l} \right) \left[1 - \frac{g \eta \eta_l}{X_{H_2O}{}^2 \varepsilon_0{}^2 u^2} \right] \right]^{\frac{1}{2}} \right) \quad \textbf{(24)}$$

$$u_i = \frac{j_v \rho_v h_{lv} - \phi_z}{(1-\varepsilon_0)\rho_d c_{p,d} \Delta T} \quad \textbf{(25)}$$

One may compare this formulation to the experimental results coming from Ginsberg [1]. The experiments considers top-reflooding of a debris bed without volumetric power. Then, on top of the flooding front, the configuration does not evolve with the height (boiling occurs at the front only). This last leads to a constant void fraction in the flooded region, hence the term $\Delta J(S^*)$ to be null, thus no capillary effect in the flooded region. In this work, this last term are also presumed to be negligible at the front itself, particularly regarding the strong boiling effects[1]. Then, for the laminar case, without heat power, the formulation reduces to:

$$u_{lam} = \frac{\rho_l g K K_{r,l} h_{lv}}{\mu_l X_{H_2O} \varepsilon h_{lv} + (1-\varepsilon_0)\rho_d Cp_d \Delta T K_{r,l} \left(\frac{\mu_v}{\rho_v K_{r,v}} + \frac{\mu_l}{\rho_l K_{r,l}} \right)} \quad \textbf{(26)}$$

Eq.(22) can be simplified since the term with X_{H2O} is quite negligible (easily verifiable), hence the front velocity can be approximated by:

$$u_{lam} \cong \frac{\phi_{l,crit}}{(1-\varepsilon_0)\rho_d c_{p,d} \Delta T}$$

So, conversely:

$$\phi_{l,crit} \cong u_{lam} (1-\varepsilon_0)\rho_d c_{p,d} \Delta T \quad \textbf{(27)}$$

This formulation points out that the quenching front velocity is directly related to the critical heat flux in a debris bed, i.e. to the critical gas flux in the flooded region. In other terms, the front propagation is limited by the flow conditions in the quenched region.

4.2. Comparison with Ginsberg Data.

Figure 4 shows the comparison of the 1D model (red curves) for a debris bed with 2D MC3D simulations (green triangles) and the experimental results from Ginsberg [1] (blue circles) at different temperatures T_0. It may be reminded that, in these experiments, the flooding occurred in two steps, first with the development of water channels that penetrate the bed. This last signifies, in essence, that the flooding occurs in a two dimensional way. However, it is estimated that these channels occupied a surface fraction of about 0.3-0.4. Thus, in the 1D model, the front velocity is expected to be lower by an inversed factor of the surface fraction (to extract the same amount of energy). As can be seen the 1D model shows the same trend as the experimental data and the MC3D calculation results, where the downward front velocity "u" decreases as the temperature increases. Considering the previous comments regarding the 2D nature of the flow in the experiments, one may conclude that the front velocity is slightly overestimated, except at low temperatures

[1] The known formulations for le Leverett J function are probably not applicable in this region.

(low ΔT with respect to T_{sat}). The MC3D calculations reproduces qualitatively well the experiments, except for the case at low permeability and high temperatures. The reason of this discrepancy is to be investigated further.

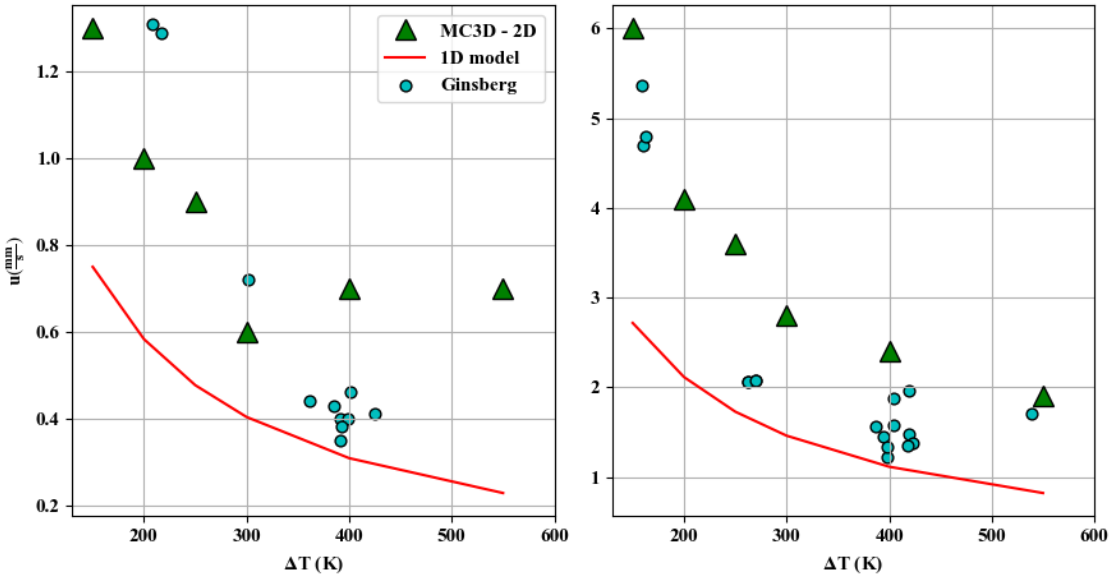

Figure 4. Ginsberg et al. [4] vs. MC3D 2D simulations and 1D model; left: d_p=0.89 mm, Zbed=0.4m, ε=0.403, and eq.(23); right: d_p=3.18 mm, Zbed=0.3m, ε=0.401, and eq.(24) & eq.(25)

4.3. Application to SSWICS Experiments

A special expected configuration of porous media is the so-called fractured corium crust. In this case, the average permeability of such media (as found in the SSWICS experiments) tends to be lower than 1E-9m^2. The crust is assumed to be relatively hot, but colder than the solidification temperature of the specific material. For such configuration, the water of the overlaying pool must first penetrate this hot material and later continue the solidification of the melt pool found underneath. In the absence of residual power in the crust, the heat extracted from this crust would come from the cooling of such material via vaporization of the infiltrated water. Shown in **Table III** are expressions to evaluate the relative permeabilities developed in the context of fractured porous media, which depend on the fluids properties, or effective saturation.

Table III. Relative Permeabilities formulas for fractured porous media

Author	$K_{r,l}$	$K_{r,v}$
Brooks & Corey[26]	$(1-S^*)^4$	$(1-S^*)^2(1-S^{*2})$
Fourar & Lenormand [27]	$\frac{(1-\alpha)^2}{2}(3-(1-\alpha))$	$\alpha^3+\frac{3\mu_v}{2\mu_l}\alpha(1-\alpha^2)$
Chima & Geiger [28]	$\frac{(1-\alpha)^2}{2}\left(\frac{2}{3}(1-\alpha)^2+(1-\alpha)\alpha\right)$	$\frac{\alpha^2}{2}\left(\frac{1}{3}\alpha^2+\frac{1\mu_v}{2\mu_l}(1-\alpha)^2+\frac{\mu_v}{\mu_l}\alpha(1-\alpha)\right)$

The front velocity is not known in these experiments, however, in application of the eq. (27), the extracted heat flux is close to the critical heat flux that may be obtained in a porous media with the same permeability. So, eq.(16) can be directly used to estimate the heat flux extracted during the penetration (capillarity should not play an important role).

Figure 5 shows the results of two SSWICS tests and eq.(16). The solid black line uses for the relative permeabilities the formulation presented in **Table I** with the Reed coefficients. The dashed lines plot eq.(16) using the relative permeabilities in **Table III**. As can be seen, all formulations of the relative permeabilities, except Chima & Geiger, lead to similar results compared to the formulation presented in **Table I**.

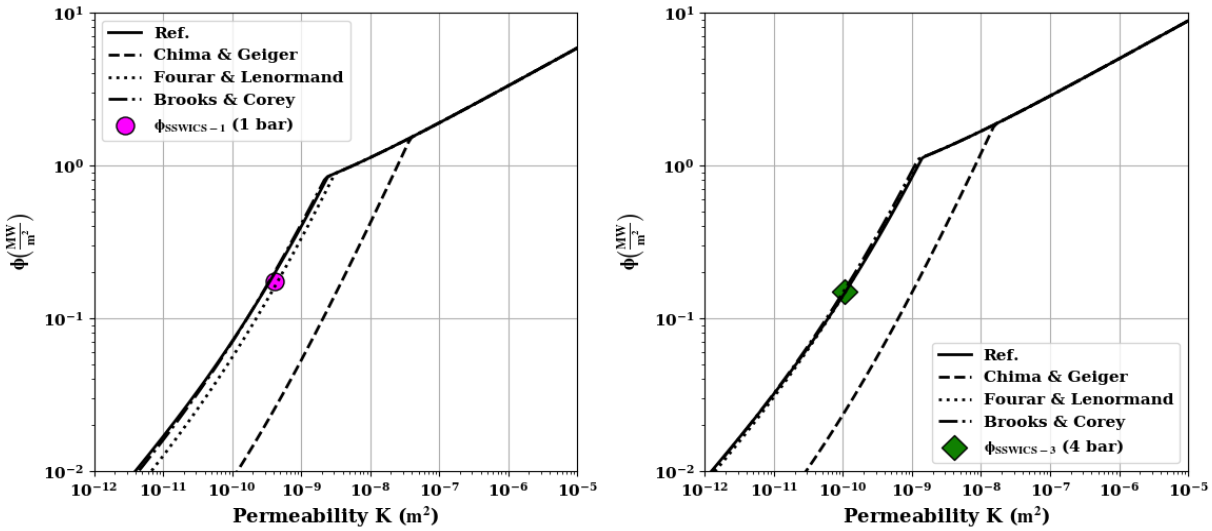

Figure 5. ϕ_{crit} compared to SSWICS W-I

5. CONCLUSIONS

The present work was realized to improve understanding and predictability of the debris bed re-flooding from the top, with special attention to the case of fractured media for application to ex-vessel corium stabilization studies. First, the problem of the stability of a flooded porous medium was revisited, highlighting the mechanisms of critical heat flux. Eq.(12) and eq.(16) are then proposed respectively for laminar and inertial regimes. The problem of top re-flooding was analyzed through the use of the CFD code, MC3D, and the development of an analytical 1D model. The MC3D calculations indicate that the water penetrates with a local 2-phase flow configuration (through the fingers). The void saturation in this 2-phase flow is found to be coherent with the critical flow conditions, i.e, at low pressure, about 75 %. The downward penetration velocity is found in acceptable agreement with the experiments for both models, thus leading to the possibilities for extrapolations to evaluate the coolability of such porous media.

It was also found that the quenching front velocity is directly related to the critical heat flux in a debris bed, i.e. to the critical gas flux in the flooded region. In other terms, the front propagation is limited by the flow conditions in the quenched region.

The model is found applicable for the phenomenon of water ingression compact fractured crust of solidified corium, a problem encountered in the severe accident phenomenology.

The precise description of the flow configuration, i.e. fingering, is still to be clarified; this could be obtained by an improvement of the CFD model (refinement of the friction model and convection model). Furthermore, an improvement of the analytical model to describe a 2D configuration is underway. Nevertheless, it is important to highlight that dedicated experimental data of re-flooding with hot-dry-heated debris bed and fractured crust is crucially needed to complement and assess the models.

6. REFERENCES

1. T. Ginsberg *et al.*, "An Experimental and analytical investigation of quenching of superheated debris bed under top-reflood conditions. Final Report," NUREG/CR-4493, (1986).
2. D. H. Cho, D. R. Armstrong, and S. H. Chan, "On the Pattern of Water Penetration into a Hot Particle Bed," *Nuclear Technology*, **65**(1), pp. 23–31 (1984).
3. M. T. Farmer, S. Lomperski, D. J. Kilsdonk, and R. W. Aeschlimann, "OECD MCCI Project Final Report," *OECD/MCCI-2005-TR06*, 2006.
4. R. J. Glass and M. J. Nicholl, "Physics of gravity fingering of immiscible fluids within porous media: An overview of current understanding and selected complicating factors," *Geoderma*, **70**(2–4), pp. 133–163 (1996).
5. S. W. Jones, M. Epstein, S. G. Bankoff, and D. R. Pedersen, "Dryout heat fluxes in particulate beds heated through the base," *Journal of heat transfer*, vol. 106, no. 1, pp. 176–183, 1984.
6. M. Epstein, "Dryout Heat Flux During Penetration of Water Into Solidifying Rock," *Journal of Heat Transfer*, vol. 128, no. 8, p. 847, 2006.
7. B. Raverdy, R. Meignen, L. Piar, S. Picchi, and T. Janin, "Capabilities of MC3D to investigate the coolability of corium debris beds," *Nuclear Engineering and Design*, **319**, pp. 48–60 (2017).
8. Kokalj Janez, Uršič Mitja, Leskovar Matjaž, Piar Libuse, and Meignen Renaud, "Modelling of debris bed reflooding in PEARL experimental facility with MC3D code," *Nuclear Engineering and Design*, **330**, pp. 450–462 (2018).
9. R. Meignen, S. Picchi, J. Lamome, B. Raverdy, S. C. Escobar, and G. Nicaise, "The challenge of modeling fuel coolant interaction: Part I – Premixing," *Nuclear Engineering and Design*, **280**, pp. 511–527 (2014)
10. P.G. Saffman and G.I. Taylor, "The penetration of a fluid into a porous medium or Hele-Shaw cell containing a more viscous liquid," *Proceedings of the Royal Society of London. Series A. Mathematical and Physical Sciences*, **245**(1242), pp. 312–329 (1958).
11. R. Clavier, "Étude expérimentale et modélisation des pertes de pression lors du renoyage d'un lit de débris," Dissertation PhD, Institut National Polytechnique de Toulouse, (2015).
12. S. Ergun, "Fluid Flow through Packed Columns," *Journal of Chemical Engineering Progress*, **48**(2), pp. 89–94 (1952).
13. R. J. Lipinski, "Model for boiling and dryout in particle beds," Sandia National Labs., NUREG/CR--2646, (1982).
14. A. W. Reed, "The effect of channeling on the dryout of heated particulate beds immersed in a liquid pool," Dissertation PhD, Massachusetts Institute of Technology, (1982).
15. K. Hu and T. G. Theofanous, "On the measurement and mechanism of dryout in volumetrically heated coarse particle beds," *International journal of multiphase flow*, **17**(4), pp. 519–532 (1991)
16. F. A. . Dullien, C. Zarcone, I. F. Macdonald, A. Collins, and R. D. . Bochard, "The effects of surface roughness on the capillary pressure curves and the heights of capillary rise in glass bead packs," *Journal of Colloid and Interface Science*, **127**(2), pp. 362–372 (1989).
17. M. Kaviany, *Principles of Heat Transfer in Porous Media*, ch..8, Springer US, New York, NY (1991).
18. M. C. Leverett, "Capillary Behavior in Porous Solids," *Transactions of the AIME*, **142**(01), pp. 152–169 (1941).

19. K. S. Udell, “Heat transfer in porous media considering phase change and capillarity—the heat pipe effect,” *International Journal of Heat and Mass Transfer*, **28**(2), pp. 485–495 (1985).
20. M. T. van Genuchten, “A Closed-form Equation for Predicting the Hydraulic Conductivity of Unsaturated Soils1,” *Soil Science Society of America Journal*, **44** (5), p. 892 (1980).
21. G. Hofmann, “On the Location and Mechanisms of Dryout in Top-Fed and Bottom-Fed Particulate Beds,” *Nuclear Technology*, **65**(1), pp. 36–45 (1984).
22. K. Miyazaki, K. Murai, T. Ohama, N. Yamaoka, and S. Inoue, “Dryout Heat Flux for Core Debris Bed, (I): Effects of System Pressure and Particle Size,” *Journal of Nuclear Science and Technology*, **23**(8), pp. 702–710 (1986).
23. L. Barleon, K. Thomauske, and H. Werle, “Cooling of Debris Beds,” *Nuclear Technology*, **65**(1), pp. 67–86 (1984).
24. K. Atkhen and G. Berthoud, “SILFIDE experiment: Coolability in a volumetrically heated debris bed,” *Nuclear Engineering and Design*, **236**(19–21), pp. 2126–2134 (2006).
25. D. Squarer, A. T. Pieczynski, and L. E. Hochreiter, “Effect of Debris Bed Pressure, Particle Size, and Distribution on Degraded Nuclear Reactor Core Coolability,” *Nuclear Science and Engineering*, **80**(1), pp. 2–13 (1982).
26. R. H. Brooks, A. T. Corey, Colorado State University, and Hydrology and Water Resources Program, *Hydraulic properties of porous media*. Colorado State University, Fort Collins, Colorado (1964).
27. M. Fourar and R. Lenormand, “A new model for two-phase flows at high velocities through porous media and fractures,” *Journal of Petroleum Science and Engineering*, **30**(2), pp. 121–127 (2001).
28. A. Chima and S. Geiger, “An Analytical Equation to Predict Gas/Water Relative Permeability Curves in Fractures.,” in *SPE Latin America and Caribbean Petroleum Engineering Conference*, Mexico City, Mexico (2012).